

Herschel observations of the Centaurus cluster, the dynamics of cold gas in a cool core



R. Mittal¹, J. B. R. Oonk², A. C. Edge³, G. Ferland⁴, C. P. O'Dea¹, and 13 other collaborators

¹Rochester Institute of Technology, ²Netherlands Institute for Radio Astronomy, ³Durham University, ⁴University of Kentucky

rmittal@astro.rit.edu

Abstract

Brightest cluster galaxies (BCGs) in the cores of galaxy clusters have distinctly different properties from other low redshift massive ellipticals. The majority of the BCGs in cool-core clusters show signs of active star formation. We present observations of NGC 4696, the BCG of the Centaurus galaxy cluster, at far-infrared (FIR) wavelengths with the Herschel space telescope.

Introduction

Recent high-resolution XMM-Newton and Chandra observations have shown that the cooling rates at the center of galaxy clusters are below the simple cooling-flow models by an order of magnitude (e.g. McNamara & Nulsen 2007). Despite AGN and other sources of heating which stop the intracluster-medium (ICM) from cooling catastrophically, observations of many (~ 40) BCGs show that the intracluster medium gas is cooling but at a much suppressed level. They appear to have substantial amount of cold gas, of which a small fraction is forming stars (e.g., Johnstone et al. 1987; McNamara et al. 1989; Edge & Frayer 2003).

A significant number of cool-core clusters show the $H\alpha$ optical line-filaments. In addition, detections of the 10^6 K optical coronal line emission [FeX] λ 6374Å (Canning et al. 2010), warm molecular H_2 at ~ 2000 K (e.g. Jaffe & Bremer 1997; Donahue et al. 2000), cold molecular H_2 at (300-400) K (Johnstone et al. 2007) and cold CO gas at few tens of kelvin (Edge 2001) imply that there is gas at almost every temperature in the range varying from the virial temperature of the ICM (10^7 K) to the temperature of the star-forming clouds (10 K). These emissions are very likely due to the gas being reheated rather than cooling out of the ICM. Understanding the details of how the mass and energy transfer occurs is crucial. To that end a key component is the molecular gas and dust at < 60 K, whose natural emission is accessible by *Herschel*.

Observations

We used the ESA Herschel space observatory (Pilbratt et al. 2010) using PACS (Poglitsch et al. 2010) and SPIRE (Griffin et al. 2010) to study the cold phase (< 60 K) of the interstellar and intracluster medium. The aim of these observations was to understand the details of mass and energy transfer between the different phases of gas. We observed the two primary coolants of the neutral ISM, the [CII] line at $157.74 \mu\text{m}$ and the [OI] line at $63.18 \mu\text{m}$, along with [OIB] at $145.52 \mu\text{m}$, [SII] at $68.470 \mu\text{m}$, [NII] at $121.90 \mu\text{m}$ and [OIII] at $88.36 \mu\text{m}$ with the PACS spectrometer. We also conducted PACS and SPIRE photometry at $70 \mu\text{m}$, $100 \mu\text{m}$, $160 \mu\text{m}$, $250 \mu\text{m}$, $350 \mu\text{m}$ and $500 \mu\text{m}$.

Results

Of the lines observed, we detected [OI], [CII] and [NII] in NGC 4696 (Fig. 1). We did not detect [SII], [OIII] and [OIB]. We also detected dust emission at all six PACS and SPIRE wavebands.

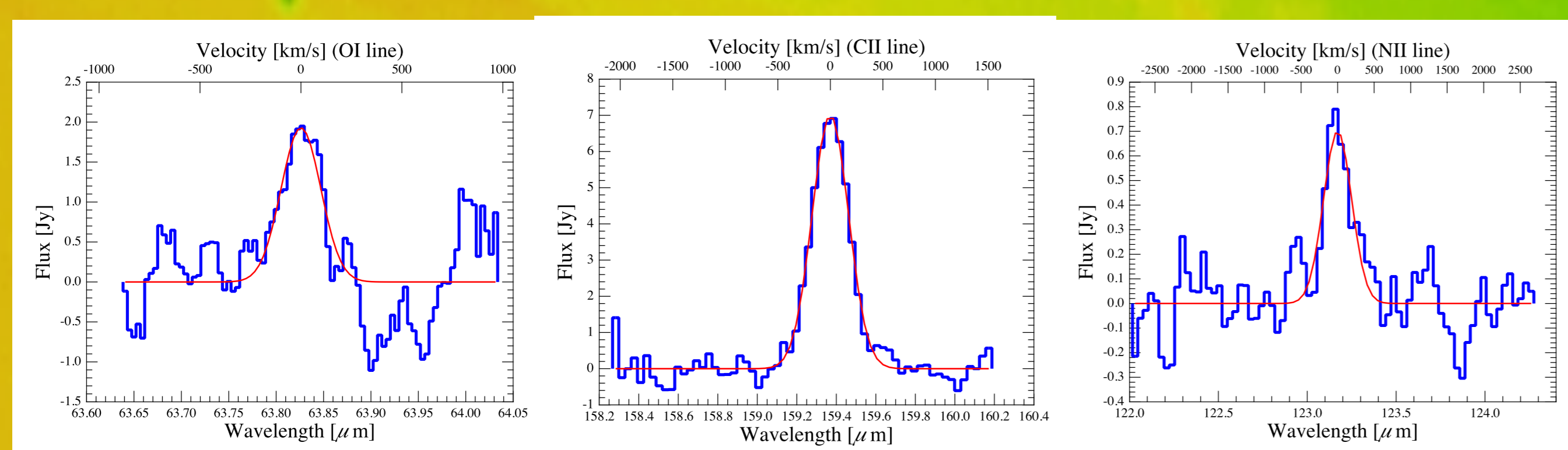


Figure 1: The forbidden FIR line detections in the center of NGC 4696.

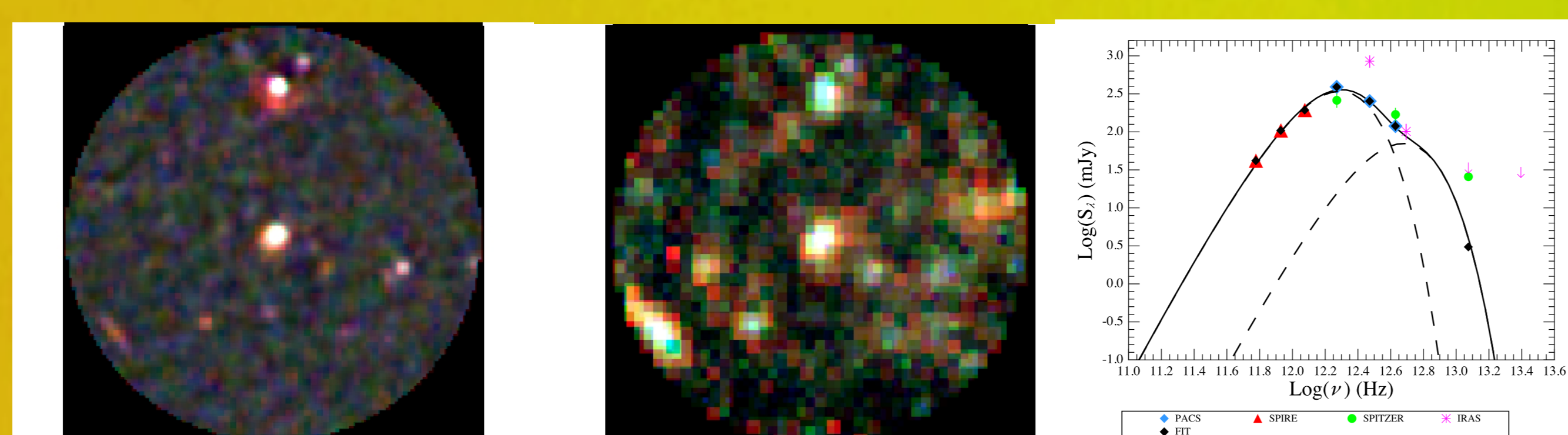


Figure 2: Photometry images of NGC 4696. Left: PACS colour images at $70 \mu\text{m}$ (blue), $100 \mu\text{m}$ (green) and $160 \mu\text{m}$ (red) combined with the same smoothing gaussian of FWHM $12''$. Middle: SPIRE colour images at $250 \mu\text{m}$ (blue), $350 \mu\text{m}$ (green) and $500 \mu\text{m}$ (red) with a resolution of $18''$, $24''$ and $38''$ respectively. The image units are Jy/beam and each side measures $7'$. Right: The FIR spectral energy distribution obtained from a modified two-component blackbody fit to the Herschel and Spitzer data.

X-ray, optical and far-infrared correlations

The morphological and kinematical correlation between the far-infrared forbidden line coolant, [CII], and the optical line filaments is a key result of this work (see Fig. 3). This correlation has a profound implication, namely that the optical hydrogen recombination line,

$H\alpha$, the optical forbidden lines, [NII] λ 6583Å, the soft X-ray filaments and the far-infrared [CII] line all have the same energy source.

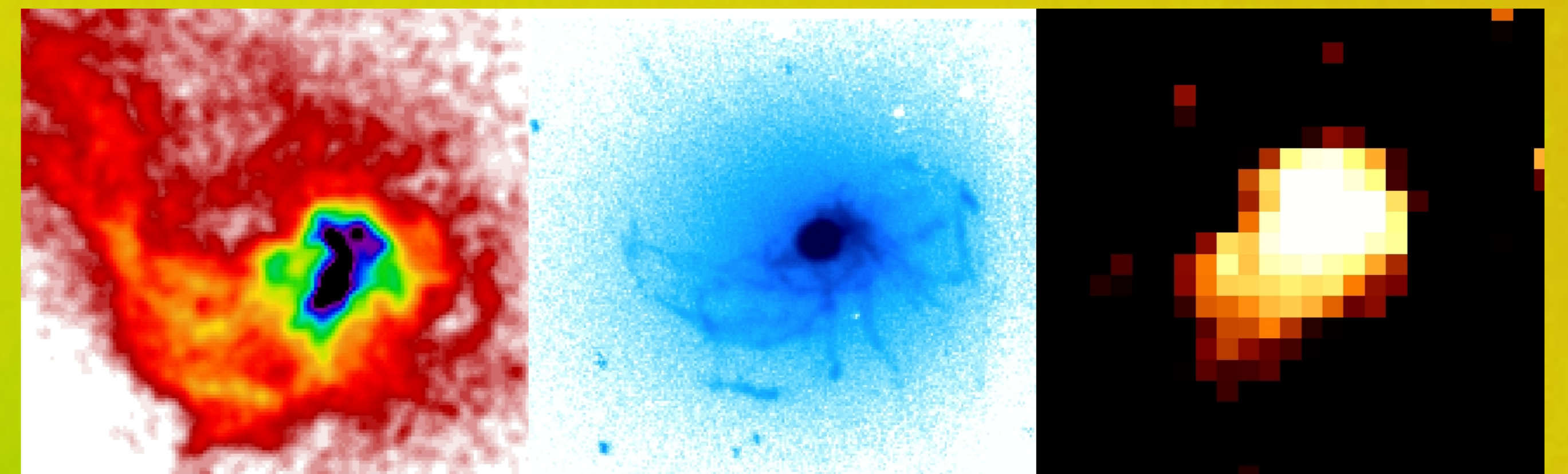


Figure 3: Soft Chandra X-ray image (left), Gemini optical $H\alpha$ emission (middle) Crawford et al. (2005) and Herschel far-infrared [CII] $157.74 \mu\text{m}$ emission (right).

Modelling of the ISM of NGC 4696

To understand the complete picture giving rise to emission in NGC 4696 at different wavebands, we performed simulations to investigate the physical parameters of its ISM using the spectral synthesis code, CLOUDY (Ferland et al. 1998).

These simulations help us to narrow down the most probable heating scenario such that it simultaneously reproduces all the observed line and continuum ratios. The best-fitting model contains photoionization from old and young stellar populations, and an additional source of heating (Table 1). Photoionization from young stars is still of paramount importance. A model containing only extra heating and no young stars produces very little [CII] because of severe lack on FUV photons. The model containing stars and "extra-heating" best explains the observations yielding a density, n , in the range of about a few tens to hundred per cm^3 and a radiation field, G_0 , in the range ten Habing to ~ 80 Habing. This range of G_0 corresponds to a star formation rate of $(0.02 \text{ to } 0.13) M_{\odot} \text{ yr}^{-1}$ for a cloud of an effective radius of 0.5 kpc . "extra-heating" may be imputed to non-radiative heating sources, like cosmic rays or magneto-hydrodynamic waves (such as those observed in the ISM of our galaxy).

Table 1: The basic photodissociation region (PDR) model parameters. The geometry is assumed to be plane-parallel. Columns: (1) parameter, (2) symbol, (3) the input range and (4) the most likely parameter values.

Parameter	Symbol	Input Range	Likely Values
Total Hydrogen Density (cm^{-3})	n	10 to 10^6	50 to 100
FUV Intensity Field (Habing*)	G_0	1 to 10^6	10 to 80
Extra Heating ($\text{erg s}^{-1} \text{cm}^{-3}$)	H_{extra}	10^{-24} to 10^{-20}	$\sim 10^{-22}$
Normalization for the OSP* ($10^{-16} \text{ erg s}^{-1} \text{cm}^{-2} \text{Hz}^{-1}$)	η_{OSP}	2.4 to 156.7	2.4
Hydrogen Column Density (cm^{-2})	N_{H}	10^{19} to 10^{23}	10^{21}
Metallicity	Z	1 – 4	2.5
Nitrogen abundance (relative to Z)	$Z_{\odot}(\text{N})$	2 – 2.5	2

* 1 Habing = $1.6 \times 10^{-3} \text{ erg s}^{-1} \text{cm}^{-2}$, OSP: Old Stellar Population

Conclusions

We performed a detailed spectral energy distribution fitting using a two-component modified black-body function and found a cold 19 K dust component with mass $1.7 \times 10^6 M_{\odot}$ and a warm 46 K dust component with mass $4.0 \times 10^3 M_{\odot}$. The total FIR luminosity between $8 \mu\text{m}$ and $1000 \mu\text{m}$ is $7.5 \times 10^8 L_{\odot}$, which using Kennicutt relation yields a low star formation rate of $0.13 M_{\odot} \text{ yr}^{-1}$. This value is consistent with values derived from other tracers, such as ultraviolet emission. Combining the spectroscopic and photometric results together with optical $H\alpha$, we modeled emitting clouds consisting of photodissociation regions (PDRs) adjacent to ionized regions. We showed that in addition to old and young stellar populations, there is another source of energy, such as cosmic rays, shocks or reconnection diffusion, required to excite the $H\alpha$ and [CII] filaments.

Acknowledgements

We would like to thank the HSC and NHSC consortium for support with data reduction pipelines.

References

- Canning, R. E. A., Fabian, A. C., Johnstone, R. M., et al. 2010, MNRAS, 1800
 Crawford, C. S., Hatch, N. A., Fabian, A. C., & Sanders, J. S. 2005, MNRAS, 363, 216
 Donahue, M., Mack, J., Voit, G. M., et al. 2000, ApJ, 545, 670
 Edge, A. C. 2001, MNRAS, 328, 762
 Edge, A. C. & Frayer, D. T. 2003, ApJ, 594, L13
 Ferland, G. J., Korista, K. T., Verner, D. A., et al. 1998, PASP, 110, 761
 Griffin, M. J., Abergel, A., Abreu, A., et al. 2010, A&A, 518, L3+
 Jaffe, W. & Bremer, M. N. 1997, MNRAS, 284, L1
 Johnstone, R. M., Fabian, A. C., & Nulsen, P. E. J. 1987, MNRAS, 224, 75
 Johnstone, R. M., Hatch, N. A., Ferland, G. J., et al. 2007, MNRAS, 382, 1246
 McNamara, B. R. & Nulsen, P. E. J. 2007, ARA&A, 45, 117
 McNamara, B. R. et al. 1989, AJ, 98, 2018
 Pilbratt, G. L., Riedinger, J. R., Passvogel, T., et al. 2010, A&A, 518, L1+
 Poglitsch, A., Waelkens, C., Geis, N., et al. 2010, A&A, 518, L2+